Magnetic and Magnetotransport Properties of Erbium Silicide Epitaxial Films

J. A. Chroboczek,[1] A. Briggs,[2] W. Joss,[3] S. Auffret,[2] and J. Pierre[2]
[1]*Centre National d'Etudes des Télécommunications, 38243 Meylan, France*
[2]*Centre National de la Recherche Scientifique, 38042 Grenoble, France*
[3]*Hochfeld-Magnetlabor, Max-Planck Institut für Festkörperforschung, 38042 Grenoble, France*
(Received 20 June 1990)

Hexagonal Er_3Si_5 films epitaxially grown on Si show strong anisotropies in magnetization and magnetotransport below the ordering temperature. The magnetoresistance has a cusplike positive anomaly or is negative and featureless for a magnetic field applied, respectively, along or perpendicular to the [0001] axis. A noncollinear structure, composed of an antiferromagnetic and a ferromagnetic component accounts for the magnetization data. The latter used in conjunction with the Yamada-Takada theory of magnetotransport accounts for the magnetoresistance data.

PACS numbers: 73.60.Aq, 72.15.Qm, 75.30.Cr, 75.50.Rr

The recent surge of interest in Er-doped solids and in silicides or pnictides of Er can be traced to two facts. First, Er as an impurity in semiconductors and insulators has been demonstrated[1] to luminesce in the 1.5-μm wavelength band,[2] important for silica fiber communications. Second, silicides of Er [and also of other rare-earth (RE) elements] and Er pnictides have been shown to form epitaxial, metallic films on Si (Refs. 3 and 4) and the III-V semiconductors,[5,6] respectively. The films have an unquestionable potential for device applications, as they combine epitaxial properties with metallic conduction, being important for both interconnections and heterojunctions on semiconductors. However, technological progress is hindered by difficulties that might be inherent in the material properties of RE compounds. For example, defect formation in Er silicide might be related to the Si vacancy ordering reported in this and other hexagonal silicides.[4,7,8] A need of a better understanding of basic properties of the RE compounds, given their potential for technological applications, explains the considerable activity in this field of materials research.

In this Letter we address the problem of magnetoresistance (MR) anomalies, originating from the interactions between magnetic moments of Er ions with electron spins.[4-6,9] The anomalies resulting from the divergence of the spin fluctuations at the ordering temperature have been discussed by de Gennes and Friedel[10] and by Fisher and Langer.[11] The anomalies we observe occur, however, below the spin-ordering temperature T_c, and are in some cases more pronounced at $T \ll T_c$. The MR anomalies below T_c have been studied in ErAs by Allen *et al.*,[5] who attributed them to electron scattering at the antiferromagnetic-paramagnetic phase boundary, where the magnetic field induces a suppression of the antiferromagnetic component of the magnetic structure. The MR anomalies in ErAs and in Er silicide originate from the same phenomenon, related to the antiferromagnetic component in their structures. However, while the structure of RE pnictides is cubic, that of RE silicides is hexagonal and, consequently, anisotropic. We find a signature of the magnetic structure anisotropy in the magnetotransport and magnetic properties of Er silicide. This makes it easier to distinguish the spin-dependent scattering effects from others and to compare them with theory. We show that predictions of the theoretical work of Yamada and Takada (YT),[12] treating the MR effects in antiferromagnetic systems, account satisfactorily for our data.

The samples used in this work were prepared[4] by the Molecular Beam Epitaxy group of the Centre National d'Etudes des Télécommunications (CNET), Meylan. The electrical transport data, temperature dependence of resistance R and of the Hall coefficient R_H, and, in particular, their variation near T_c (found to be about 4.3 K), have been discussed earlier.[4] This work is restricted to Er_3Si_5, as it was found that the silicide of this stoichiometry had the best overall electrical and structural properties, probably because of a periodic arrangement

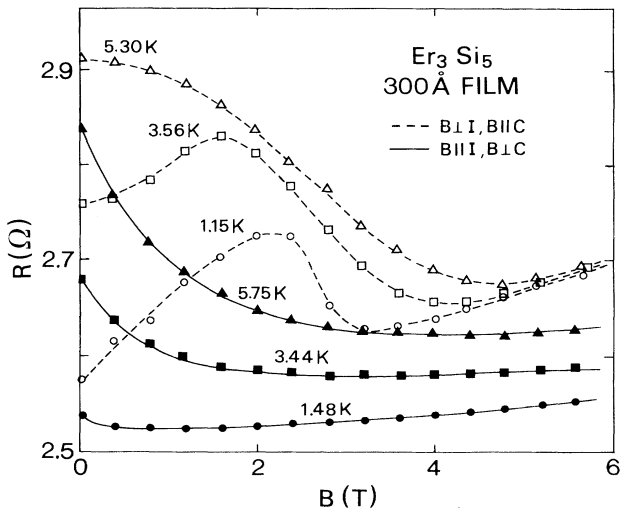

FIG. 1. Transverse (open data points) and longitudinal (solid points) magnetoresistance with the current I applied along the [11$\bar{2}$0] orientation. The lines serve to guide the eye.

of Si vacancies.[4,7] Figure 1 shows that at $T < T_c$ the transverse MR ($B \| c \perp I$, where c is the hexagonal axis normal to the basal plane and I is the current) has a cusplike anomaly at $B \approx 2$ T, followed by an increase (orbital MR), visible at $B > 4$ T. Interestingly, the increase was found to be linear in B up to 22 T (not shown), which suggests the open-orbit transport. This fact is consistent with the observations[4] that R_H can change sign when the temperature is varied. The longitudinal MR ($B \| I \perp c$) is a featureless function of B, with a rapid drop observed at low-field strengths (solid points and solid lines in Fig. 1).

Crucial to the understanding of the MR were the magnetization data. They were collected, by means of the SQUID technique, on a stack of oriented film samples (total silicide mass of about 0.1 mg). The temperature dependence of the inverse magnetic susceptibility $1/\chi$ was found to follow the Curie-Weiss law for $T > 50$ K, with a paramagnetic moment equal to the free Er^{+3}-ion value and a Néel temperature equal to -16 K; its low-temperature variation is shown in the inset in Fig. 2. Note that $1/\chi$ has a minimum at T_c for $B \| c$, while for $B \perp c$ it drops to zero at T_c. Therefore, for these two B orientations the system behaves, respectively, as an antiferromagnet and a ferromagnet. Magnetization data for $B \| c$ indicate a metamagnetic behavior at $T < T_c$, leading to a ferromagnetic saturation at $B \approx 3$ T, with a saturation moment of $7.5\mu_B$ per Er^{+3} ion. For $B \perp c$, a spontaneous magnetization (about $2.5\mu_B$/ion at 1.6 K) is observed and found to increase with the field, reaching $3.6\mu_B$ at 7 T.

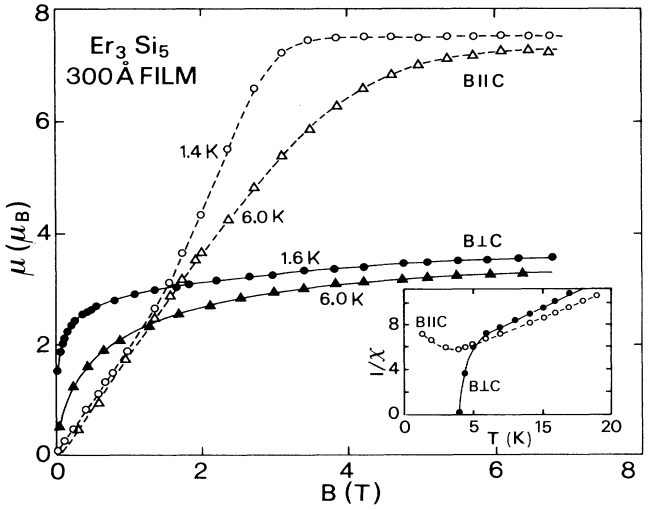

FIG. 2. Magnetization as a function of the magnetic field for two different orientations (open and solid symbols), each for a temperature above and below the ordering temperature T_c. Inset: The dependence of the inverse magnetic susceptibility on temperature for the two orientations of the magnetic field, for the field strength extrapolated to zero. The lines serve to guide the eye.

We found that the magnetization data taken on a bulk, Czochralski-grown, monocrystal of Er_3Si_5 showed the same general behavior as that of film specimens. We could therefore assume that neutron-scattering data obtained on bulk material, in a parallel study,[13] were relevant for the film samples. The magnetic structure consists of a ferromagnetic and an antiferromagnetic component arranged noncollinearly. The ferromagnetic component is composed of $1.7\mu_B$ moments lying in the basal planes. The moments forming the antiferromagnetic component have a length of $5.7\mu_B$ and are aligned, parallel or antiparallel, to the c axis. Consulting Ref. 13 might be helpful for understanding the geometry of the magnetic structure. The structure accounts satisfactorily for the magnetization data shown in Fig. 2: For $B \perp c$ (here $B \| [11\bar{2}0]$, and lower curves in Fig. 2) the moments are tilted towards the field orientation, whereas $B \| c$ (upper curves) induces the metamagnetism and leads to a higher saturation value of the magnetization, consistent with the fact that the initial antiferromagnetic component is aligned along the c axis. In addition, due to the anisotropy of the $4f$ wave function of the Er^{+3} ion, the length of the total magnetic moment of the ions decreases with the angle it forms with the c axis. These magnetization data served to establish the crystal-field (CF) parameters and the exchange parameters, assuming that the structure is described by two sublattices (referred to below as A and B). The fitting procedure will be discussed in detail elsewhere. We found that the CF parameters, $B_2^0 = -0.15 \pm 0.05$ K, $B_4^0 = 0.0026 \pm 0.0005$ K, $B_6^0 = 10^{-5} \pm 5\times10^{-6}$ K, and $B_6^6 = 2\times10^{-4} \pm 10^{-4}$ K account satisfactorily for the excitation inelastic-neutron-scattering spectra, paramagnetic susceptibility, and the magnetization data (Fig. 2). The exchange parameters were set in order to account for the magnitude of T_c, the antiferromagnetic coupling between the c-axis components M_A^z, M_B^z ($n_{AA}^z = 0$, $n_{AB}^z = -0.16$ K), and the ferromagnetic coupling between the basal-plane components M_A^x, M_B^x ($n_{AA}^x = n_{AB}^x = 0.16$ K). The calculated dependence of magnetization for $B \| [11\bar{2}0]$ and $B \| [0001]$ is presented in Fig. 3 for temperatures corresponding (approximately) to those used in Fig. 2. A quantitative agreement between the two sets of plots is evident. At this stage, however, we did not attempt to reach a closer agreement, since the calculated magnetization accounted in a satisfactory manner for the MR behavior at $T < T_c$ in the framework of the YT theory.[12]

Yamada and Takada[12] have calculated the resistivity from the spin-correlation function. Two terms related to the longitudinal and transverse spin fluctuations have been derived as functions of the total magnetic field, as well as the magnitude of the magnetic moment and its field derivative for each sublattice [cf., Eqs. (3.9) and (3.10) of YT]. The theory[12] can be applied to RE silicides with some modifications. First, the magnetocrystalline anisotropy has to be taken into account as it is involved in the magnetic energy in the direction of the mo-

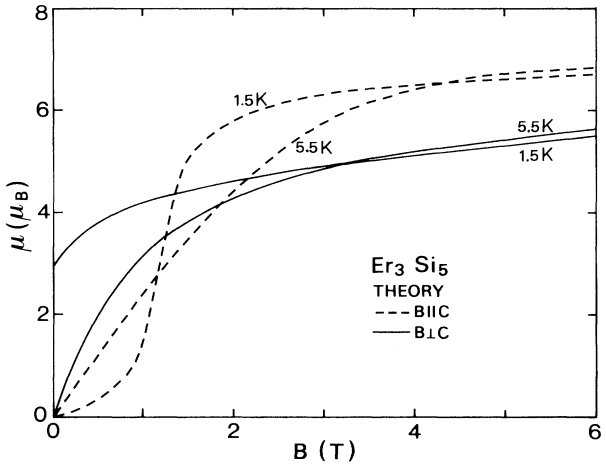

FIG. 3. Magnetization curves computed according to the calculations of Yamada and Takada for 1.5 and 5.5 K with the magnetic field applied parallel and perpendicular to the c axis of the structure. The crystal-field parameters used are given in the text; the exchange parameters have been chosen to account for the magnitude of the ordering temperature and the magnetic structure.

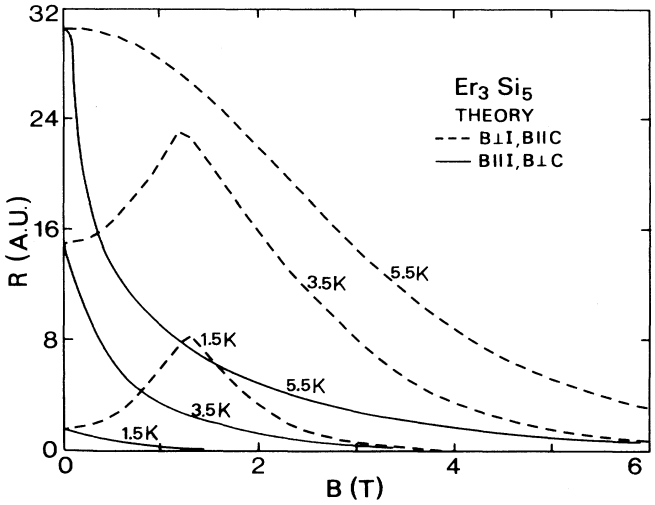

FIG. 4. Magnetoresistance computed with the same parameters as those used for computing the magnetization dependence on the magnetic-field strength shown in Fig. 3.

ments and in the spin-correlation function. Second, the assumption of a constant magnitude of the magnetic moments cannot be applied to Er_3Si_5, as the moments have been shown to decrease when tilted towards the basal plane. With the correct description of magnetic energies and moments, the YT theory accounts qualitatively for the negative longitudinal MR and for the cusplike anomaly for B parallel to the spin axis of the antiferromagnetic component. The curves shown in Fig. 4 represent the MR dependence calculated for temperatures close to those used for the data shown in Fig. 3.

The salient features of the transverse MR data can be explained now in a simple manner. For uniaxial antiferromagnets, the metamagnetic behavior of the magnetization for a field along the direction of moments implies a transition from a periodic, antiferromagnetic structure, to another periodic, but ferromagnetic structure, when the total field acting on one of the spin sublattices, equal to $B-B_{ex}$, changes sign (here B_{ex} is the exchange field). The sign reversal of the total field acting on this sublattice reduces the level splitting to zero, which corresponds to the maximum electron scattering, hence the resistance maximum. Note that for Er_3Si_5 the MR maximum (Figs. 1 and 4) moves to higher values of B as T decreases, as required by the corresponding increase in B_{ex}. The maximum disorder should then occur at the midrise field in the magnetization curve at a corresponding temperature, a fact corroborated by the experimental data in Figs. 1 and 2, and reproduced by the calculation, as shown in Figs. 3 and 4.

The longitudinal MR data are also satisfactorily accounted for by calculation; it is negative and featureless throughout the whole field range of Figs. 1 and 4. At $T \ll T_c$ the negative component is small and the entire resistance change occurs in the field region where magnetization increases rapidly, due to the alignment and saturation of the ferromagnetic component of the structure. The longitudinal MR is more pronounced at higher temperatures, where the thermal spin fluctuations are stronger; the magnetic field suppresses the latter by increasing the splitting between the spin-up and spin-down states. The form of the longitudinal MR in the ordered state can be more readily understood if the MR in the paramagnetic state ($T \gg T_c$) is first analyzed.

At $T \gg T_c$ and with $B \| I$ (configuration minimizing the positive, orbital component of the MR) the longitudinal MR has a well-known sigmoidal form, horizontal at the origin, then decreasing, and finally saturating at a sufficiently strong B. We fitted the data taken at 10 and 20 K, for $B \| [11\bar{2}0]$, for two different Er_3Si_5 film samples, using the expression[5,10,11]

$$R = R_0 + R_s[\tfrac{3}{4} - \tfrac{1}{4}\tanh^2(gB\mu_B/2kT)]\,; \qquad (1)$$

thus treating the Er moments as spin-$\frac{1}{2}$ particles with an effective magnetic moment $(g/2)\mu_B$. The constant R_s depends on the band-structure parameters: electron density, Fermi momentum vector, and also the scattering cross section for the s-d interaction.[5,10,11] Note that the magnetic induction B in Eq. (1) should incorporate B_{ex}; thus,

$$B = B_{appl} + B_{ex} = B_{appl}[1 + T_c/(T - T_c)]\,. \qquad (2)$$

From the fit of the four longitudinal MR data sets, we obtained $\mu = (g/2)\mu_B = (3.6 \pm 0.2)\mu_B$, a value which agrees perfectly with the magnetization at saturation,

shown in Fig. 2, for the same field orientation. Because of a complicated relation between the Fermi vector and the electron density, R_s cannot be expressed in simple terms and the analysis is restricted to the g values extracted from the fit. However, R_s was found to increase as T was lowered, a feature consistent with the variation of R_H, reported previously.[4]

Returning now to the discussion of the longitudinal MR in the ordered phase, we should bear in mind that the magnetic induction acting on the ions is equal to B_{ex} for a vanishing external field. Thus the longitudinal MR curve can be obtained from the sigmoidal MR curve in the paramagnetic state by a shift in the origin by the amount B_{ex} along the magnetic-field axis. Therefore the MR curve starts with a negative slope, and the net variation diminishes with increasing $gB\mu_B/2kT$, as shown in Fig. 1. However, the initial dip at low B can be attributed to the ferromagnetic component ordering [with the corresponding instantaneous increase in magnetization (Figs. 2 and 3)]. So far we have no explanation of the increase in the longitudinal MR, clearly visible at the lowest curve in Fig. 1.

Summarizing, the quantitative fit of the MR in the paramagnetic phase has given the value of the magnetic moment of Er ground state, consistent with the independent measurement of magnetization. The MR in the ordered phase is qualitatively described by the YT theory,[12] which (1) reproduces the positive, cusplike anomaly seen in MR for $B\|c$, (2) gives negative and featureless MR for $B\perp c$, and (3) correlates the prominent features in the magnetic-field dependences of MR and magnetization.

This study has evolved from the silicide research program of the Materiaux Actifs pour Dispositifs Department, CNET, Meylan. Continuous interactions with our colleagues from CNET were invaluable for the development of this work.

[1]H. Ennen, J. Schneider, G. Pomrenke, and A. Axmann, Appl. Phys. Lett. **43**, 943 (1983).

[2]For review, see F. Auzel, in *French-Israeli Workshop on Solid State Lasers,* edited by G. Boulon, C. K. Jorgesen, and R. Reisfeld (Society of Photo-Optical Instrumentation Engineers, Bellingham, WA, 1988).

[3]J. E. Baglin, F. M. Huerle, and C. S. Petersson, J. Electrochem. Soc. **126**, 154 (1979).

[4]F. Arnaud d'Avitaya, P. A. Badoz, Y. Campidelli, J. A. Chroboczek, J. Y. Duboz, and A. Perio, Thin Solid Films **184**, 283 (1990).

[5]S. J. Allen, N. Tabatabaie, C. J. Palmstrom, G. W. Hull, T. Sands, F. DeRosa, H. L. Gilchrist, and K. C. Garrison, Phys. Rev. Lett. **62**, 2309 (1989).

[6]A. Guivarc'h, A. LeCorre, J. Caulet, B. Guenais, M. Minier, G. Ropars, P. A. Badoz, and J. Y. Duboz, Mater. Res. Soc. Symp. Proc. **160**, 331 (1990); also J. A. Chroboczek *et al.*, in Proceedings of the Twentieth International Conference on the Physics of Semiconductors, Thessaloniki, 1990 (to be published).

[7]J.A. Knapp and S. T. Picraux, Appl. Phys. Lett. **48**, 466 (1986).

[8]R. Baptist, S. Ferrer, G. Grenet, and H. C. Poon, Phys. Rev. Lett. **64**, 311 (1990).

[9]L. D. Woolf, Solid State Commun. **47**, 519 (1833), and references therein.

[10]P. G. de Gennes and J. Friedel, J. Phys. Chem. Solids **4**, 71 (1958).

[11]M. F. Fisher and J. S. Langer, Phys. Rev. Lett. **20**, 665 (1968).

[12]H. Yamada and S. Takada, J. Phys. Soc. Jpn. **34**, 51 (1973).

[13]S. Auffret, J. Pierre, B. Lambert, J. L. Soubeyroux, and J. A. Chroboczek, Physica (Amsterdam) **162B**, 271 (1990).